

Overall elastoplastic property for micropolar composites with randomly oriented ellipsoidal inclusions

Hansong Ma, Xiaoning Liu, Gengkai Hu *

Department of Applied Mechanics, Beijing Institute of Technology, 100081 Beijing, China

Received 21 June 2005; received in revised form 13 December 2005; accepted 13 December 2005

Abstract

Overall linear and non-linear properties for micropolar composites containing 3D and in-plane randomly oriented inclusions are examined with an analytical micromechanical method. This method is based on Eshelby solution for a general ellipsoidal inclusion in a micropolar media and secant moduli method. The influence of inclusion's shape, size and orientation on the classical effective moduli, yielding surface and non-linear stress and strain relation are examined. The results show that the effective moduli and non-linear stress–strain curves are always higher for micropolar composites than the corresponding classical composites. When the inclusion's size is sufficiently large, the classical results can be recovered.

© 2005 Elsevier B.V. All rights reserved.

Keywords: Micropolar theory; Composite; Micromechanics; Plasticity

1. Introduction

During the past decades, size-dependence of material behavior was confirmed repeatedly by experiment and becomes an important fact in engineering design. The most known experiences are that for some tiny structures, the dimensionless torsion or bending response becomes stiffer when the size of the structures is reduced [1]. Heterogeneous materials (composites or polycrystalline metals) exhibit another kind of size effect: when size of constituents is refined, the overall properties are strengthened [2]. These two different but relevant size-related phenomena have the same origin in nature: that is, when the characteristic size of structure or microstructure is small, non-local effect becomes important [3]. This paper aims at the second size-dependence phenomenon, especially for fiber-reinforced composites.

To establish relation between overall property of composites and their constituents, micromechanical methods

were particularly developed; many micromechanical models have been proposed. Briefly, they fall into the following four groups: (a) Universal rigorous principles for composites whatever the involved microstructure of the composite, this is due to CLM theorem [4]. (b) Bounding methods, by which the range of overall property can be estimated with limited microstructural information [5,6]. (c) Approximate methods, where complex interaction of phases is replaced by certain simple pattern, then such single pattern is embedded in a reference material to build localization relation. Mori–Tanaka's mean field method, self-consistent and generalized self-consistent method or double inclusion methods are the known examples, see more details in the monograph given by Nemat-Nasser and Hori [5]. Their interconnection is established recently by Hu and Weng [7]. (d) Computational methods, where a sample of microstructure is realized and whole solution is obtained through numerical discretization [8]. However, since taking Cauchy continuum model (any surface of an infinitesimal material element transmits only force, not couple) as its background, none of the mentioned methods can take size parameter into account.

* Corresponding author. Fax: +86 10 68914780.

E-mail address: hugeng@bit.edu.cn (G. Hu).

To include the size effect into a continue formulation, many efforts have been made to remedy the traditional continuum theory; such theory is usually referred as *high order continue theory*. In this paper, micropolar theory termed by Eringen [9] is utilized as a basic high order continuum description for matrix material response. For a micropolar material, each material point can experience not only translation but also independent rigid rotation. This theory is relevant for granular materials, polycrystalline or multi-molecular bodies. Muhlhaus and Vardoulakis [10], de Borst [11] have constructed micropolar plasticity theory for studying strain localization phenomenon. If more independent degrees of freedom are introduced to describe the response of a material point, more complex theories can be obtained, namely, microstretch, micromorphic [12]. In addition, Fleck and Hutchinson [13] and Gao et al. [15] proposed a strain gradient theory, and Aifantis [14] proposed a gradient plasticity theory, the two theories can also describe the well-observed size effect. All of the mentioned high order theories introduce some intrinsic length parameters, however their determination remains unsolved.

As concerning as predicting the size-dependence of composite materials, much works have been conducted recently. There are two different approaches to tackle these problems, one is based on strain gradient theory or its modification; the other is based on micropolar theory. Smyshlyaev and Fleck [16,17] used strain gradient theory to bound or estimate the effective elastic and plastic behavior of composite with strain gradient effect, Fleck and Willis [18] evaluated effective plastic property of isotropic composites with a modified strain gradient theory. The influence of the particle size on the overall plastic property of composite can be captured with their methods. As far as concern with micropolar theory for composite materials, Yuan and Tomita [19] evaluated the effective elastic moduli of a micropolar matrix with periodic voids; Chen and Wang [20] examined the overall non-linear properties of a micropolar composite with aligned short fibers. Both of these two works utilized finite element calculation on a periodic unit cell. Recently, efforts have been made to propose analytical micromechanical method. With help of micropolar Eshelby solutions for spherical and cylindrical inclusions given by Cheng and He [21,22], Sharma and Dasgupta [23], Liu and Hu [24] and Xun et al. [25,26] extended independently the classical Mori–Tanaka method to estimate effective elastic properties for particulate composites, as well as long fiber composites. To predict the non-linear overall properties for micropolar composites, Liu and Hu [24], Xun et al. [26] proposed an analytical micromechanical method by extending classical secant moduli scheme with second-order stress moment [27–29], and such method was further shown to have a variational structure [3] similar to Ponte Castañeda variational principle for a Cauchy composite [30]. The proposed method can also successively predict the size-dependence well observed for metal–matrix composites. Since the methods based on micropolar theory generalize directly the classical microme-

chanical methods to micropolar composite, and there are simple analytical expressions for the Eshelby tensors, so this method provides a simple alternative to predict the size effect for composite materials.

Recently, a simple form of Eshelby’s solution for a general ellipsoidal inclusion embedded in a micropolar matrix have been obtained semi-analytically by Ma and Hu [31]. Based on this solution, Ma and Hu [32] further examined the overall non-linear properties of a micropolar composite with aligned arbitrary ellipsoidal fibers, influences of aspect ratio and size of fibers were examined.

The objective of this paper is to examine overall elastoplastic properties of micropolar composites with 3-dimensional (3D) or in-plane (2D) randomly oriented ellipsoidal fibers, which is not addressed previously. The influence of fiber’s shape, size and orientation will be examined. The paper will be arranged as follows: In Section 2 a brief preliminary of micropolar theory will be recalled, Section 3 will be devoted to theoretical formulation of linear and non-linear overall properties of micropolar composites with 3D and 2D randomly oriented ellipsoidal fibers, numerical examples will be presented in Section 4 and the paper is ended by some conclusions.

2. Micropolar elasticity and plasticity

We are interested in the composite material where the coarse microstructure of matrix material must be taken into account due to the small size of inclusions. In such case the matrix is therefore idealized as a micropolar material model [3]. Before proceeding, we recall, briefly, the essential elements of micropolar theory.

In absence of body forces and couples, the governing equations of a centro-symmetric and isotropic micropolar material are [12,33]

$$\varepsilon_{ij} = u_{j,i} - e_{kij}\phi_k, \quad k_{ij} = \phi_{j,i} \quad (1a)$$

$$\sigma_{ij,i} = 0, \quad m_{ij,i} + e_{jik}\sigma_{ik} = 0 \quad (1b)$$

$$\begin{aligned} \sigma_{ji} &= \delta_{ji}\lambda\varepsilon_{kk} + (\mu + \kappa)\varepsilon_{ji} + (\mu - \kappa)\varepsilon_{ij} \\ m_{ji} &= \delta_{ji}\alpha k_{kk} + (\beta + \gamma)k_{ji} + (\beta - \gamma)k_{ij} \end{aligned} \quad (1c)$$

where σ_{ij} and m_{ij} denote the non-symmetric stress and couple stress tensors, ε_{ij} and k_{ij} non-symmetric strain and torsion tensors, u_i and ϕ_i displacement and microrotation vectors, respectively, e_{ijk} permutation tensor and δ_{ij} Kronecker delta. μ , λ are classical Lamé’s constants and κ , γ , β , α are the new elastic constants introduced in micropolar theory. The following conditions must be defined on the boundary in order to establish a well-posed problem:

$$\sigma_{ji}n_i = t_j \quad m_{ji}n_i = p_j \quad \text{on } \Gamma^\sigma \quad (2a)$$

$$u_i = \bar{u}_i \quad \phi_i = \bar{\phi}_i \quad \text{on } \Gamma^u \quad (2b)$$

Due to the dimensional difference between the two sets of moduli, three intrinsic characteristic lengths can be defined [24]:

$$l_1 = (\gamma/\mu)^{1/2}, \quad l_2 = (\beta/\mu)^{1/2}, \quad l_3 = (\alpha/\mu)^{1/2} \quad (3)$$

The constitutive equation (1c) can be rewritten in a compact form if we denote $\sigma'_{(ij)}$, $\sigma_{(ij)}$, $\sigma (\equiv \sigma_{ii})$ and $\varepsilon'_{(ij)}$, $\varepsilon_{(ij)}$, $\varepsilon (\equiv \varepsilon_{ii})$ as, respectively, the deviatoric symmetric, anti-symmetric and hydrostatic parts of the stress and strain tensors (similar notations for couple-stress and torsion tensors):

$$\sigma'_{(ij)} = 2\mu\varepsilon'_{(ij)}, \quad \sigma_{(ij)} = 2\kappa\varepsilon_{(ij)}, \quad \sigma = 3K\varepsilon, \quad (4a)$$

$$m'_{(ij)} = 2\beta k'_{(ij)}, \quad m_{(ij)} = 2\gamma k_{(ij)}, \quad m = 3Nk, \quad (4b)$$

with

$$K = \lambda + \frac{2}{3}\mu, \quad N = \alpha + \frac{2}{3}\beta, \quad (5)$$

where subscripts (\cdot) and $\langle \cdot \rangle$ denote the symmetric and anti-symmetric parts of a tensor, respectively.

Through an elaborate definition of plastic stress potential and J_2 -type effective stress, a deformation version of plasticity can be established for micropolar material [24]:

$$w = w_0(\sigma_{\text{eff}}) + \frac{1}{4\kappa}\sigma_{(ij)}\sigma_{(ij)} + \frac{1}{18K}\sigma^2 + \frac{1}{18N}m^2 \quad (6)$$

$$\sigma_{\text{eff}}^2 = \frac{3}{2}\sigma'_{(ij)}\sigma'_{(ij)} + \frac{3}{2}l^2(m'_{(ij)}m'_{(ij)} + m_{(ij)}m_{(ij)}) \quad (7)$$

where for simplicity, the characteristic lengths are assumed to be equal ($l_1 = l_2 = l_3 = l$), throughout this paper, the following power-law type hardening potential is adopted for the plastic matrix material:

$$w_0(\sigma_{\text{eff}}) = \frac{\sigma_{\text{eff}}^2}{6\mu} + \frac{n}{n+1} \frac{1}{H^{1/n}} (\sigma_{\text{eff}} - \sigma_y)^{\frac{n+1}{n}} \quad (8)$$

where σ_y , n and H are elastic limit, hardening exponent and modulus, respectively.

3. Theoretical formulation

3.1. Eshelby relations for an ellipsoidal inclusion

Suppose an infinite centro-symmetric and isotropic micropolar material characterized by moduli \mathbf{C}_0 and \mathbf{D}_0 , a fictitious domain Ω is isolated and endowed with a uniform stress-free eigenstrain ε^* and eigentorsion \mathbf{k}^* . Following Mura [34], such a domain is called an inclusion. Due to the constraint of surrounding material the induced strain and torsion by the prescribed eigenstrain and eigentorsion can be written as

$$\varepsilon(\mathbf{x}) = \mathbf{S}(\mathbf{x}) : \varepsilon^* + \mathbf{L}(\mathbf{x}) : \mathbf{k}^* \quad (9a)$$

$$\mathbf{k}(\mathbf{x}) = \hat{\mathbf{S}}(\mathbf{x}) : \varepsilon^* + \hat{\mathbf{L}}(\mathbf{x}) : \mathbf{k}^* \quad (9b)$$

where the tensors \mathbf{S} , $\hat{\mathbf{S}}$, \mathbf{L} and $\hat{\mathbf{L}}$ are called micropolar Eshelby tensors [21]. For these micropolar Eshelby tensors, Cheng and He [21,22] gave explicit solutions for a spherical and an infinite long cylinder inclusions. For a more general ellipsoidal inclusion, it is difficult to obtain a full analytical expression. Recently, Ma and Hu [31] derived semi-analytical

expressions of these tensors for a general ellipsoidal inclusion in a micropolar matrix, and the results are listed in Appendix A. Unlike classical material, the micropolar Eshelby tensors are not uniform even inside of an ellipsoidal inclusion, however the numerical computation shows that their fluctuation within an ellipsoidal inclusion is not significant [31].

Now we consider an ellipsoidal inhomogeneity featured by $(\mathbf{C}_1, \mathbf{D}_1)$ embedded in an infinite micropolar matrix $(\mathbf{C}_0, \mathbf{D}_0)$, where remote strain and torsion field \mathbf{E}_0 and \mathbf{K}_0 are applied. The average effective inclusion method (AEIM) is utilized to compute the average strain and torsion in the inhomogeneity [24], which can be expressed as follows:

$$\mathbf{C}_1(\mathbf{E}_0 + \langle \varepsilon \rangle_1) = \mathbf{C}_0(\mathbf{E}_0 + \langle \varepsilon \rangle_1 - \varepsilon^*) \quad (10a)$$

$$\mathbf{D}_1(\mathbf{K}_0 + \langle \mathbf{k} \rangle_1) = \mathbf{D}_0(\mathbf{K}_0 + \langle \mathbf{k} \rangle_1 - \mathbf{k}^*) \quad (10b)$$

To further proceed, we have to consider the average of the micropolar Eshelby relations (Eq. (9)) over the domain occupied by the inhomogeneity. It is shown that, for a general ellipsoidal inclusions, the averaged cross items in (9) vanished [31]:

$$\langle \mathbf{L} \rangle_1 = 0, \quad \langle \hat{\mathbf{S}} \rangle_1 = 0 \quad (11)$$

where $\langle \cdot \rangle_1$ means the volume average of the said quantity over the inclusion domain. The average micropolar Eshelby relations are uncoupled for a general ellipsoidal inclusion, so we have the following form:

$$\langle \varepsilon \rangle_1 = \langle \mathbf{S} \rangle_1 : \varepsilon^*, \quad \langle \mathbf{k} \rangle_1 = \langle \hat{\mathbf{L}} \rangle_1 : \mathbf{k}^* \quad (12)$$

Non-zero average micropolar Eshelby tensors $\langle \mathbf{S} \rangle_1$ and $\langle \hat{\mathbf{L}} \rangle_1$ can be obtained with the expressions given in Appendix A.

With help of Eqs. (10) and (12), the averages of the strain and torsion inside of the inhomogeneity can then be evaluated. It must be mentioned that the average effective inclusion method is approximate due to the non-uniform field inside of inhomogeneity, however it is shown that this approximation can provide an accurate average fields compared to the exact result [25].

3.2. Estimation of effective moduli for a micropolar composite

In the following, two-phase composite will be considered, where ellipsoidal fibers $(\mathbf{C}_1, \mathbf{D}_1)$ are oriented randomly in the space or randomly on a plane in the matrix $(\mathbf{C}_0, \mathbf{D}_0)$, and the volume fraction of fibers is f . As discussed previously, we are interested in the classical effective property of the composite, which are related to the average symmetric stress and strain by $\langle \varepsilon^{\text{sym}} \rangle = \mathbf{M}_c^{\text{sym}} : \langle \sigma^{\text{sym}} \rangle$. To this end, we follow the method proposed by Liu and Hu [24], and we apply a symmetric macroscopic stress Σ^{sym} on the boundary of RVE. It is shown that $\Sigma^{\text{sym}} = \langle \sigma^{\text{sym}} \rangle$, so in the following, the key point is to compute $\langle \varepsilon^{\text{sym}} \rangle$ as function of the applied macroscopic stress Σ^{sym} .

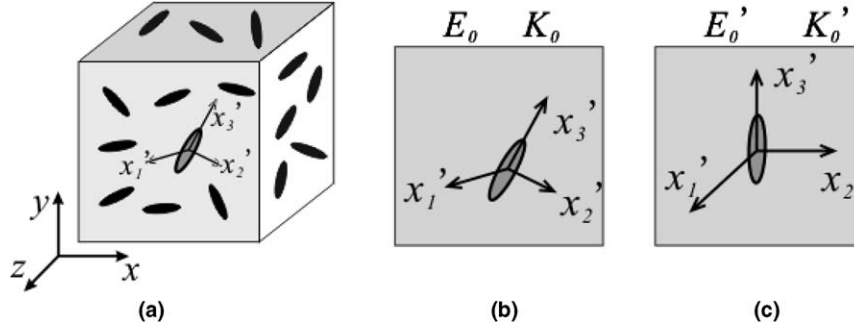


Fig. 1. Methodology of Mori–Tanaka’s method: (a) local and global frames; (b) single fiber in global system; (c) single fiber in local frame.

Consider a RVE of the composite, as shown in Fig. 1a, a local coordinate system is attached with each fiber with its three principle axes, as shown in Fig. 1b. Following the concept of Mori–Tanaka’s method [35], we place each fiber in an infinite micropolar matrix under remote yet-known applied strain and torsion \mathbf{E}'_0 and \mathbf{K}'_0 , the primed quantity means the quantity in the local coordinate system (Fig. 1c). \mathbf{E}_0 and \mathbf{K}_0 are interpreted as the average strain and torsion of the matrix in the macroscopic coordinate system.

In the local system, we apply the average effective inclusion method to determine the average strain and torsion in the fiber, this can be written as

$$\mathbf{C}'_1(\mathbf{E}'_0 + \langle \varepsilon' \rangle_1) = \mathbf{C}'_0(\mathbf{E}'_0 + \langle \varepsilon' \rangle_1 - \varepsilon^{*}) \quad (13a)$$

$$\mathbf{D}'_1(\mathbf{K}'_0 + \langle \mathbf{k}' \rangle_1) = \mathbf{D}'_0(\mathbf{K}'_0 + \langle \mathbf{k}' \rangle_1 - \mathbf{k}^{*}) \quad (13b)$$

$$\langle \varepsilon' \rangle_1 = \langle \mathbf{S} \rangle_1 : \varepsilon^{*} \quad (13c)$$

$$\langle \mathbf{k}' \rangle_1 = \langle \hat{\mathbf{L}} \rangle_1 : \mathbf{k}^{*} \quad (13d)$$

Since we are interested in the average of the symmetric strain and stress over RVE, so Eqs. (13a) and (13c) are split into a symmetric part and an anti-symmetric part, only the symmetric parts are kept in the following analysis. So the effective inclusion method can be written in this case as the following form:

$$\mathbf{C}_1^{/sym} : (\mathbf{E}_0^{/sym} + \langle \varepsilon^{/sym} \rangle_1) = \mathbf{C}_0^{/sym} : (\mathbf{E}_0^{/sym} + \langle \varepsilon^{/sym} \rangle_1 - \varepsilon^{*/sym}) \quad (14)$$

$$\langle \varepsilon^{/sym} \rangle_1 = \langle \mathbf{S}^{sym} \rangle_1 : \varepsilon^{*/sym} \quad (15)$$

where $S_{ijmn}^{sym} = (S_{ijmn} + S_{ijnm} + S_{jimn} + S_{jimm})/4$ for a fourth-order symmetric tensor and $\varepsilon_{ij}^{sym} = (\varepsilon_{ij} + \varepsilon_{ji})/2$ for a second-order tensor. Eqs. (14) and (15) allow one to determine the average symmetric strain of each fiber in the local system. In order to perform the orientational average, the strain obtained in the local system must be transformed into the global system, this can be performed by following exactly the same method as classical micromechanical method (see for example [37]). Here, the fiber is assumed to be an isotropic Cauchy material, $\mathbf{C}_1^{/sym} = \mathbf{C}_1$; the matrix material is centro-symmetric isotropic material $\mathbf{C}_0^{/sym} = \mathbf{C}_0^{sym}$, finally the classical effective compliance tensor for the micropolar composite reads

$$\mathbf{M}_c^{sym} = \mathbf{M}_0^{sym} + f[(\mathbf{M}_1 : (\mathbf{M}_0^{sym})^{-1} - \mathbf{I})^{-1} + (1-f)\langle \mathbf{I} - \langle \mathbf{S}^{sym} \rangle_1 \rangle_{\text{oriave}}]^{-1} : \mathbf{M}_0^{sym} \quad (16)$$

where \mathbf{M}_c^{sym} , \mathbf{M}_0^{sym} and \mathbf{M}_1 are the symmetric compliance tensor of the composite, matrix and fiber, respectively. \mathbf{I} is unit tensor. $\langle \cdot \rangle_{\text{oriave}}$ stands for the orientational average of the said quantity, the methods for evaluating the orientational average are given in Appendix B for 3D and 2D random orientations.

Eq. (16) has the same form as for the classical composite, size-dependence of the fiber is implicitly included in the average micropolar Eshelby tensor $\langle \mathbf{S}^{sym} \rangle_1$. It has been shown that when the fiber’s size is sufficiently large, $\langle \mathbf{S}^{sym} \rangle_1$ is reduced to the classical Eshelby tensor [31], so the classical results can be recovered.

3.3. Yield surface of micropolar composites

It is assumed that the whole composite yields when the average effective stress of matrix material reaches its elastic limit σ_y , that is

$$\langle \sigma_{\text{eff}} \rangle_0 = \sigma_y \quad (17)$$

where $\langle \cdot \rangle_0$ means the volume average of the said quantity over the matrix, and σ_{eff} is defined by Eq. (7).

In order to compute $\langle \sigma_{\text{eff}} \rangle_0$ in an analytical way, it is further assumed that $\langle \sigma_{\text{eff}} \rangle_0 \approx \sqrt{\langle \sigma_{\text{eff}}^2 \rangle_0}$, this assumption is widely accepted in micromechanics [27,29]. Following the perturbation method proposed by Liu and Hu [24], we can derive the analytical expression of $\langle \sigma_{\text{eff}}^2 \rangle_0$ as function of the applied macroscopic stress Σ^{sym} . The yielding surface of the micropolar composite can be determined with help of Eq. (17). The final expression is summarized here:

$$\frac{3}{1-f} \Sigma^{\text{sym}} : \mathbf{Q} : \Sigma^{\text{sym}} + \sigma_y^2 = 0 \quad (18)$$

$$\mathbf{Q} = \mu_0^2 \frac{\partial \mathbf{M}_c^{sym}}{\partial \mu_0} + \frac{1}{l^2} \left(\beta_0^2 \frac{\partial \mathbf{M}_c^{sym}}{\partial \beta_0} + \gamma_0^2 \frac{\partial \mathbf{M}_c^{sym}}{\partial \gamma_0} \right) \quad (19)$$

where μ_0 , β_0 , γ_0 are moduli of the micropolar matrix, \mathbf{M}_c^{sym} is determined by Eq. (16).

3.4. Non-linear stress and strain relation of micropolar composites

When the macroscopic stress exceeds the initial yielding stress of the composite, plastic deformation will take place in the matrix material. In order to model the weakened constraint power of the plastic matrix on fiber, the secant moduli method based on second-order stress and couple stress moment will be utilized in this paper [24].

For a certain plastic state of the matrix material, its secant moduli can be obtained through Eqs. (6)–(8), this leads to

$$\mu_0^s = \frac{1}{(1/\mu_0) + 3[(\sigma_{\text{eff}} - \sigma_y)/H]^{1/n}/\sigma_{\text{eff}}}, \quad \kappa_0^s = \kappa, \quad (20)$$

$$K_0^s = K_0, \quad \beta_0^s = l^2 \mu_0^s, \quad \gamma_0^s = l^2 \mu_0^s, \quad N_0^s = N_0$$

where the superscript “s” means secant quantity.

The procedure of evaluating overall non-linear stress–strain relation by secant moduli scheme is summarized as follows: for any given macroscopic stress Σ^{sym} , at which the matrix has entered into plastic state, for a tested average effective stress of the matrix $\langle \sigma_{\text{eff}} \rangle_0 (> \sigma_y)$, the secant moduli of the matrix can be evaluated by Eq. (20). We consider a linear comparison composite, it has the same microstructure and fiber’s property as the actual non-linear composite, however its matrix has the secant modulus of the actual matrix in the non-linear composite. The compliance tensors M_c^{sym} of this linear comparison composite can be determined from Eq. (16). The average effective stress of the micropolar matrix for the linear comparison composite can then be evaluated with the expression of M_c^{sym} , this provides an equation to determine for a given applied load Σ^{sym} the corresponding $\langle \sigma_{\text{eff}} \rangle_0$. The moduli of the linear comparison composite are interpreted as the secant moduli of the actual composite. By repeating Σ^{sym} , the non-linear stress and strain curves of the micropolar composite material can then be established.

4. Numerical applications

In this section some numerical calculations are performed in order to illustrate the theoretical formulations presented in Section 3. A metal–matrix composite SiC/Al is chosen as the sample material, the material constants are $\mu_0 = 26$ GPa, $\lambda_0 = 50$ GPa for the matrix and $\mu_1 = 209$ GPa, $\lambda_1 = 108$ GPa for a common fiber material (compared with rigid inclusions or voids); $\kappa_0 = 13$ GPa, $l = 10$ μm are assumed for the micropolar constants of the matrix. Other parameters will be specified when used. The geometry of a fiber is well defined by its equator radius a together with its aspect ratio ($alpha$). Here, a characterizes the size of fiber and $alpha$ its shape.

4.1. Effective elastic moduli

The composite is isotropic for a 3D composite and transversely isotropic for 2D composite (symmetry axis is

along x_1). The predicted effective shear modulus μ_c for a 3D composite, in-plane shear modulus μ_{c23} and out-of-plane shear modulus μ_{c12} for a 2D composite as function of fiber’s aspect ratio are shown in Fig. 2. The fiber’s size

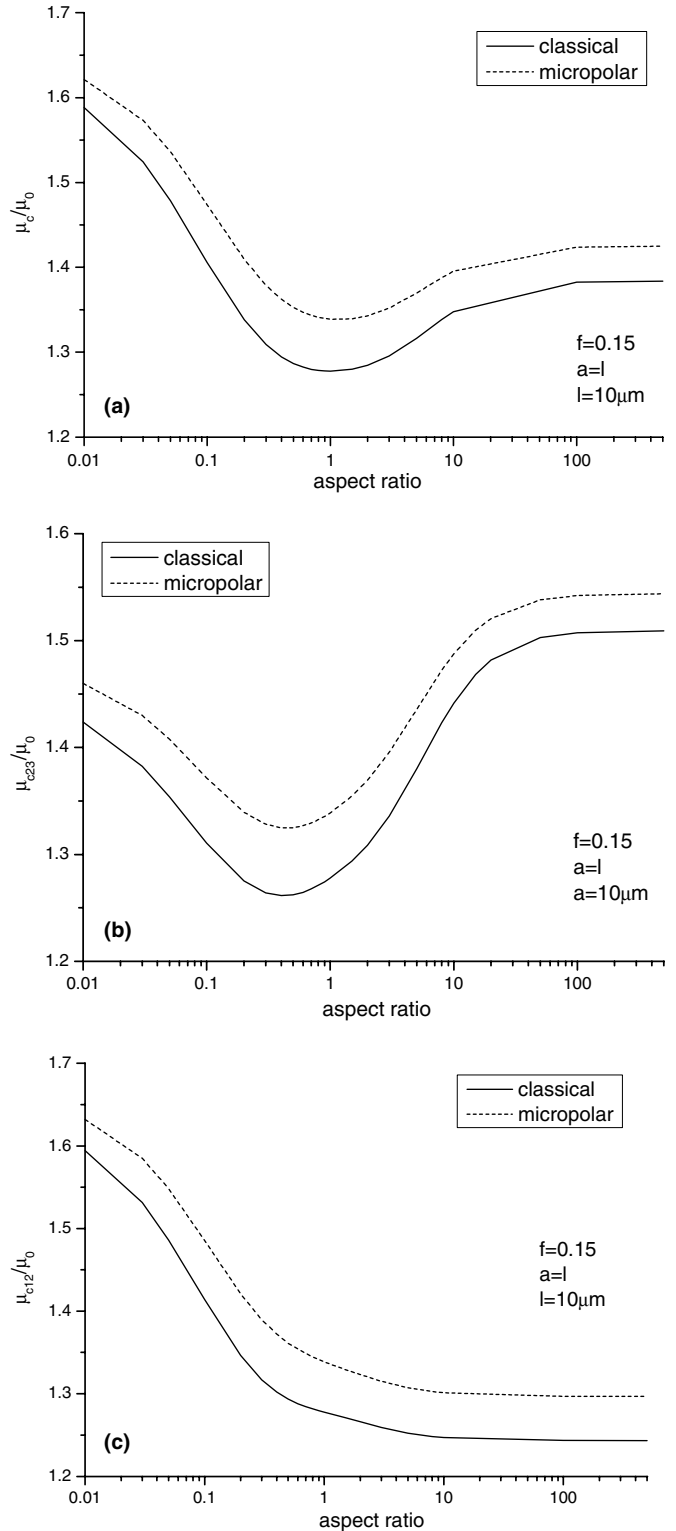


Fig. 2. Effective shear moduli as function of fiber’s aspect ratio: (a) shear moduli of 3D composite; (b) in-plane shear moduli of 2D composite; (c) out-of-plane shear moduli of 2D composite.

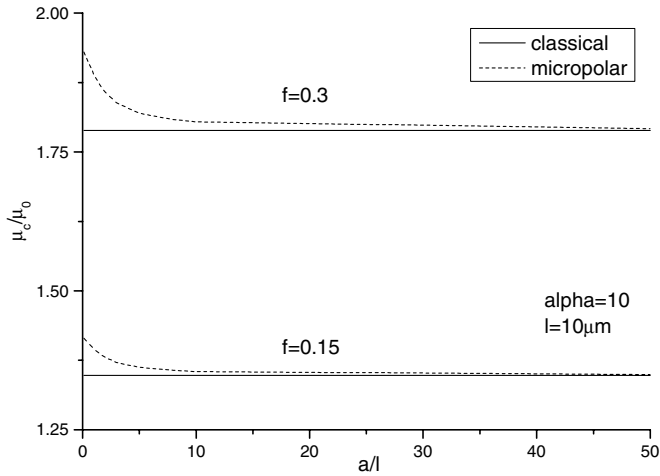


Fig. 3. Effective shear moduli for 3D-random composite as a function of fiber's size with a fixed aspect ratio 10.

is chosen to be $a = l$, its volume fraction is $f = 0.15$. For comparison, prediction by classical Mori–Tanaka's method is also included. It is found that the predicted effective shear moduli of the micropolar composites are slightly

higher than those for the classical composite, the dependence on the fiber's aspect ratio is the same for these two models.

The aspect ratio of the fiber is now kept fixed, it is taken to be 10, Fig. 3 shows the predicted effective shear modulus of 3D composite as function of fiber's size, two volume fractions $f = 0.15$ and $f = 0.3$ are examined, respectively. The classical predictions are also included for comparison. It is found that when the size of fiber is comparable or less than the intrinsic length of the matrix material, the enhancement of overall moduli is more pronounced; when the fiber's size is much larger than the intrinsic length of the matrix material, the prediction by the two theories coincides, as expected.

4.2. Initial yield surface

Fig. 4 shows the yield surfaces in $\Sigma_{33} - \Sigma_{11}$ stress-space for 3D and 2D composites for three different fiber's aspect ratios 0.2, 1 and 10, respectively. The initial yield stress of matrix is set to be $\sigma_y = 250$ MPa, the fiber is considered to be rigid, while the size and volume fraction are $a = l$ and

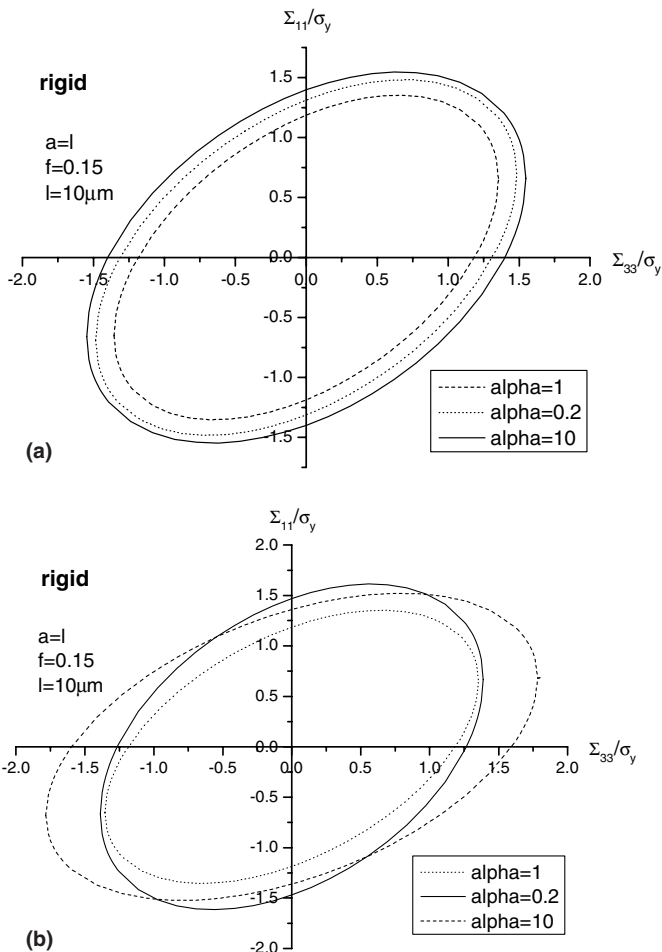


Fig. 4. Yield surfaces in $\Sigma_{33} - \Sigma_{11}$ space for rigid fiber of three different aspect ratios 0.2, 1 and 10: (a) 3D composite; (b) 2D composite.

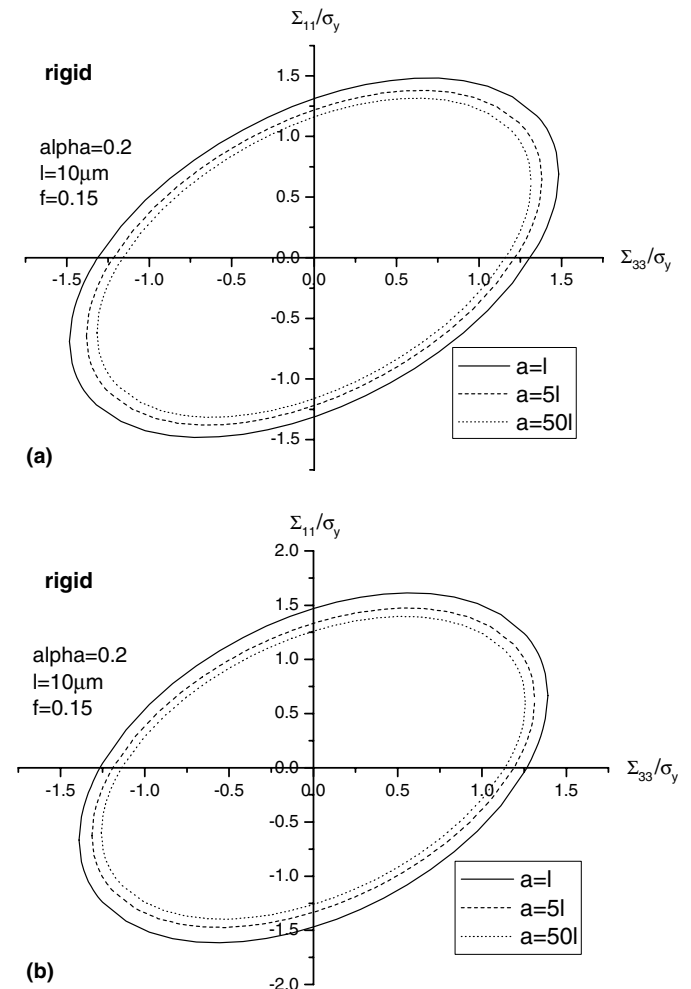


Fig. 5. Yield surfaces in $\Sigma_{33} - \Sigma_{11}$ space for rigid fiber of three different sizes: $a = l$, $a = 5l$, $a = 50l$: (a) 3D composite; (b) 2D composite.

$f = 0.15$, respectively. It can be seen from Fig. 4a that for the 3D composites the yielding surfaces are enlarged uniformly when the aspect ratio of fiber is different from unity, due to its overall isotropy. On the other hand for the 2D composite, the rotation of the yield surface is observed, as shown in Fig. 4b.

Fig. 5 presents the yield surfaces in $\Sigma_{33} - \Sigma_{11}$ space for both types of composites (3D and 2D composites) with $f = 0.15$, aspect ratio of the rigid fiber is fixed as 0.2, three different fiber's sizes $a = l$, $a = 5l$, $a = 50l$ are examined. It is found that when the fiber's size decreases, the yield surface of the composite is slightly enlarged uniformly for both types of composites. Further calculations with different fiber's properties reveal that the influence of fiber's aspect ratio and size on the overall properties is more pronounced when the stiffness of fiber becomes large.

4.3. Non-linear stress and strain relation

Non-linear overall stress–strain curve of the micropolar composite will be estimated under uniaxial loading along

x_3 . The plastic parameters of the matrix are $\sigma_y = 250$ MPa, $h = 173$ MPa and $n = 0.455$, which corresponds to Al matrix.

The influence of fiber's aspect ratio on the overall stress–strain curves is illustrated in Fig. 6 for the both types of composites, the common fiber with aspect ratios 0.01, 0.1, 1, 10, 100 are examined. The fiber's size is set to be $a = l$ and volume fraction $f = 0.15$. It is found that fiber's shape has a significant influence on the stress and strain relation for the micropolar composite, the same as for the corresponding Cauchy composite. Now the aspect ratio of fiber is fixed to be 0.2, the other material constants remain unchanged, the stress–strain curves of the both composites with three different fiber's sizes: $a = l$, $a = 5l$ and $a = 50l$ are examined, which are shown in Fig. 7. The predictions for the composite with the classical matrix and the stress and strain relation of the un-reinforced matrix are also included for comparison. The results show that the influence of fiber's size is also important, especially when the fiber's size approaches to the characteristic length of the matrix material. However

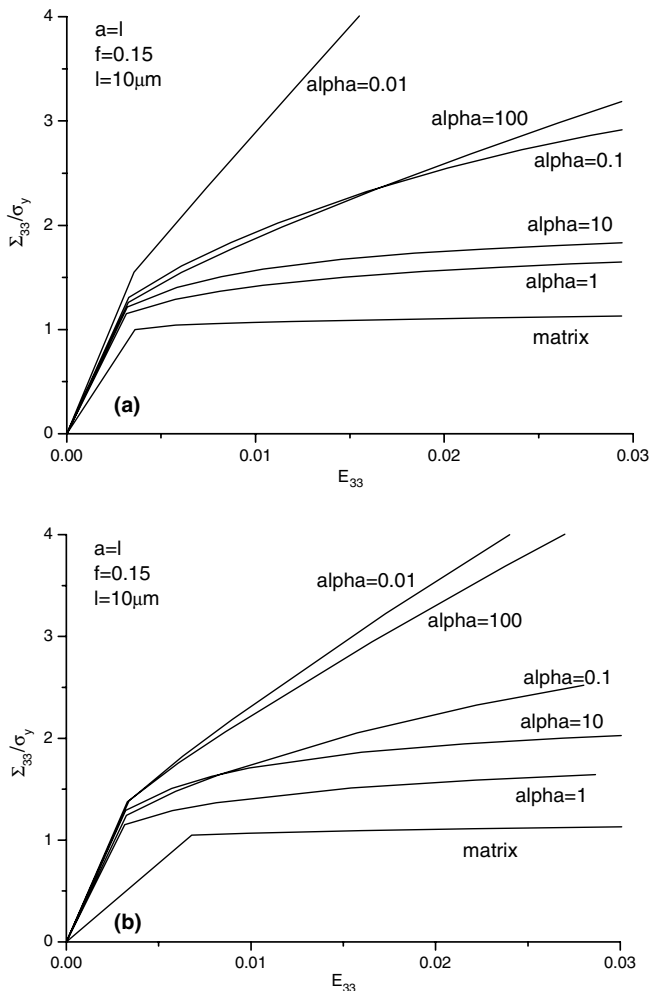


Fig. 6. Overall stress–strain relations for common inclusion with different aspect ratios: (a) 3D composite; (b) 2D composite.

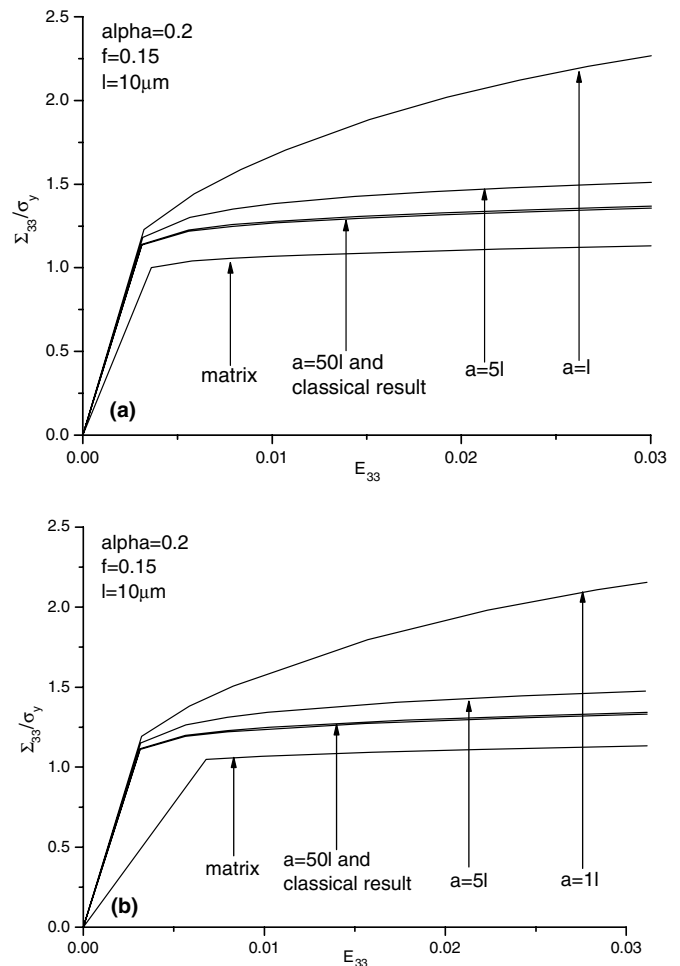


Fig. 7. Overall stress–strain relations for common inclusion with different sizes: (a) 3D composite; (b) 2D composite.

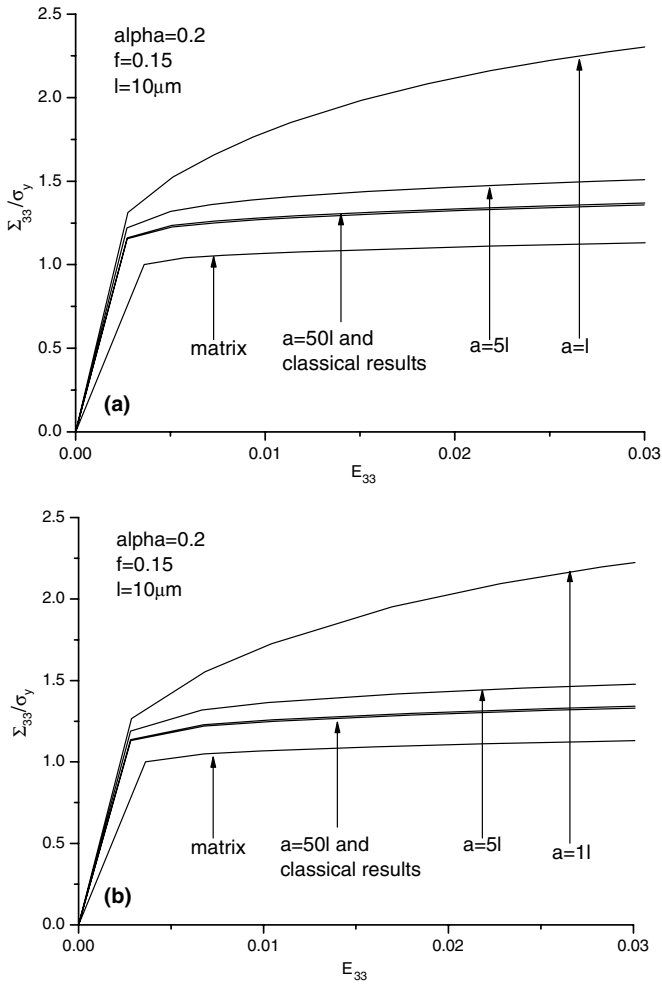


Fig. 8. Overall stress–strain relations for rigid inclusion with different sizes: (a) 3D composite; (b) 2D composite.

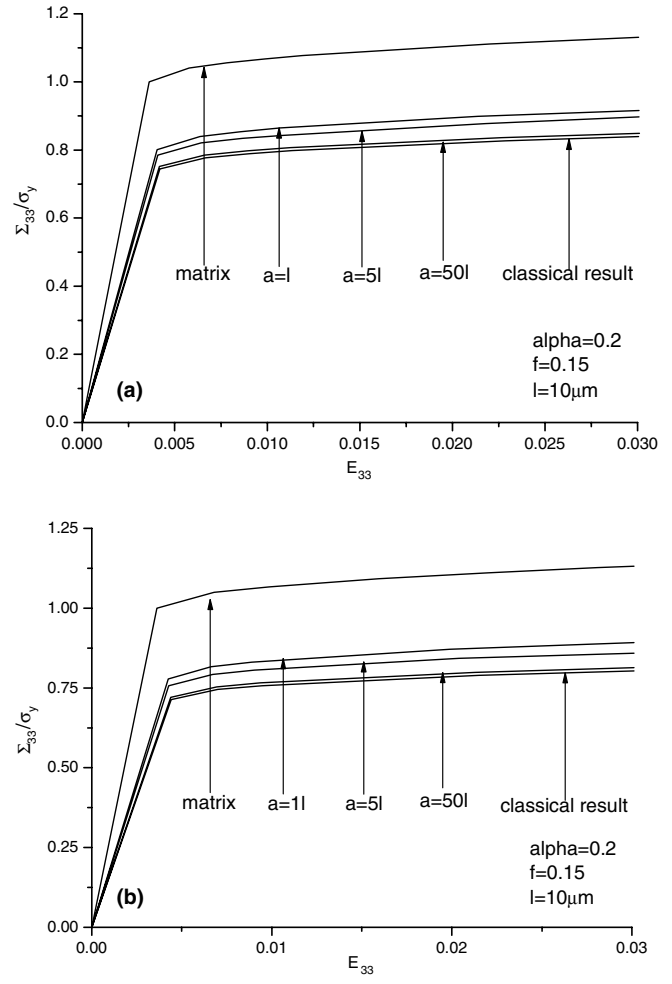


Fig. 9. Overall stress–strain relations for voids with different size: (a) 3D composite; (b) 2D composite.

when the fiber’s size is large, the predicted results by the current method is reduced to the classical one as it should be.

Analogous to Fig. 7, all other parameters are unchanged, but the fiber’s properties are replaced with two limit properties, say, rigid and void ellipsoids. Figs. 8 and 9 show the stress–strain curves with rigid and void inclusions, respectively, both 3D and 2D composites are calculated. We find that for small size of inclusions the composites are more strengthened by rigid inclusions, and relatively less weakened by voids. Furthermore, the size-dependence on overall property is much less significant for void inclusions, compared to the rigid inclusions. Again, when the inclusion’s size tends to infinity, classical results are found.

5. Conclusions

In this paper, the matrix material is idealized as a micropolar continue model. Based on Eshelby solutions for a

general ellipsoidal inclusion in micropolar media, together with Mori–Tanaka concept and secant moduli method, the overall linear and non-linear properties of metal–matrix composites containing three dimensionally or in-plane randomly oriented inclusions are examined. The classical effective moduli, initial yield surface and the effective plastic stress and strain relation are evaluated and analyzed in detail. The results show that the effective moduli and non-linear stress and strain curves are always higher, and the influence of inclusion’s aspect ratio are always more significant, than those based on classical material model, especially for small size of inclusions. When the inclusion’s size is sufficiently large, the classical results can be found.

Acknowledgement

This work is supported by the National Natural Science Foundation of China under Grant Nos. 10325210 and 10332020.

Appendix A. Eshelby tensor for an ellipsoidal inclusion [31]

The expressions of micropolar Eshelby tensors are listed here [21,31]:

$$S_{mnji}(\mathbf{x}) = I_{nji,m}^S(\mathbf{x}) + I_{nji,m}(\mathbf{x}) - e_{lmn}\hat{I}_{lji}(\mathbf{x}) \quad (\text{A.1a})$$

$$L_{mnji}(\mathbf{x}) = J_{nji,m}(\mathbf{x}) - e_{lmn}\hat{J}_{lji}(\mathbf{x}) \quad (\text{A.1b})$$

$$\hat{S}_{mnji}(\mathbf{x}) = \hat{I}_{nji,m}(\mathbf{x}) \quad (\text{A.1c})$$

$$\hat{L}_{mnji}(\mathbf{x}) = \hat{J}_{nji,m}(\mathbf{x}) \quad (\text{A.1d})$$

where

$$I_{nji}^S = \frac{\lambda + \mu}{\lambda + 2\mu}\psi_{,ijn}(\mathbf{x}) - \frac{\lambda}{\lambda + 2\mu}\delta_{ij}\phi_{,n}(\mathbf{x}) - \delta_{in}\phi_{,j}(\mathbf{x}) - \delta_{jn}\phi_{,i}(\mathbf{x})$$

$$\begin{aligned} I_{nji} &= 2Ph^2\mu\phi_{,ijn}(\mathbf{x}) + \frac{2\kappa}{\mu}[\delta_{jn}\phi_{,i}(\mathbf{x}) - \delta_{in}\phi_{,j}(\mathbf{x})] \\ &\quad - Ph^2[\lambda\delta_{ij}M_{,kkn}(\mathbf{x}, h) + 2\mu M_{,ijn}(\mathbf{x}, h)] + P\lambda\delta_{ij}M_{,n}(\mathbf{x}, h) \\ &\quad + \left[P(\mu + \kappa) + \frac{\kappa}{\mu} \right] \delta_{in}M_{,j}(\mathbf{x}, h) \\ &\quad + \left[P(\mu - \kappa) - \frac{\kappa}{\mu} \right] \delta_{jn}M_{,i}(\mathbf{x}, h) \end{aligned}$$

$$\begin{aligned} J_{nji}(\mathbf{x}) &= -\frac{1}{2\mu}[(\beta + \gamma)e_{nik}\phi_{,jk}(\mathbf{x}) + (\beta - \gamma)e_{njik}\phi_{,ik}(\mathbf{x})] \\ &\quad + \frac{1}{2\mu}[(\beta + \gamma)e_{nik}M_{,jk}(\mathbf{x}, h) + (\beta - \gamma)e_{njik}M_{,ik}(\mathbf{x}, h)] \end{aligned}$$

$$\begin{aligned} \hat{I}_{nji}(\mathbf{x}) &= \frac{1}{2\mu}[\kappa e_{ijk}\phi_{,kn}(\mathbf{x}) - (\mu + \kappa)e_{nik}\phi_{,kj}(\mathbf{x}) \\ &\quad - (\mu - \kappa)e_{njik}\phi_{,ki}(\mathbf{x})] - \frac{1}{2\mu}[(\mu + \kappa)e_{ijk}M_{,kn}(\mathbf{x}, h) \\ &\quad - (\mu + \kappa)e_{nik}M_{,kj}(\mathbf{x}, h) - (\mu - \kappa)e_{njik}M_{,ki}(\mathbf{x}, h)] \\ &\quad + \frac{1}{2}e_{ijk}M_{,kn}(\mathbf{x}, g) + \frac{\mu + \kappa}{2\mu h^2}e_{ijn}M(\mathbf{x}, h) \end{aligned}$$

$$\begin{aligned} \hat{J}_{nji}(\mathbf{x}) &= -\frac{\beta}{2\mu}\phi_{,ijn}(\mathbf{x}) + \frac{\mu + \kappa}{4\mu\kappa}[\alpha\delta_{ij}M_{,kkn}(\mathbf{x}, h) + 2\beta M_{,ijn}(\mathbf{x}, h)] \\ &\quad - \frac{1}{4\kappa}[\alpha\delta_{ij}M_{,kkn}(\mathbf{x}, g) + 2\beta M_{,ijn}(\mathbf{x}, g)] \\ &\quad - \frac{\mu + \kappa}{4\mu\kappa h^2}[\alpha\delta_{ij}M_{,n}(\mathbf{x}, h) + (\beta + \gamma)\delta_{in}M_{,j}(\mathbf{x}, h) \\ &\quad + (\beta - \gamma)\delta_{jn}M_{,i}(\mathbf{x}, h)] \end{aligned}$$

$$P = \kappa/[\mu(\mu + \kappa)], \quad h^2 = \frac{(\mu + \kappa)(\gamma + \beta)}{4\mu\kappa}, \quad g^2 = \frac{(\alpha + 2\beta)}{4\kappa}$$

Evaluation of the micropolar Eshelby tensors depends on the following three integrals and their spatial derivatives, which are defined by

$$\begin{aligned} \psi(\mathbf{x}) &= \frac{1}{4\pi} \int_{\Omega} x \, d\mathbf{x}', \quad \phi(\mathbf{x}) = \frac{1}{4\pi} \int_{\Omega} \frac{1}{x} \, d\mathbf{x}', \\ M(\mathbf{x}, k) &= \frac{1}{4\pi} \int_{\Omega} \frac{e^{-x/k}}{x} \, d\mathbf{x}' \end{aligned} \quad (\text{A.2})$$

where $x = |\mathbf{x}|$.

For a general ellipsoidal inclusion, $\psi(\mathbf{x})$ and $\phi(\mathbf{x})$ have been integrated analytically [34], while analytical expression of $M(\mathbf{x}, k)$ is almost hopeless. However, it can be reduced to the following 1D integral:

$$M(\mathbf{x}, k) = \frac{1}{4\pi} \int_{\Omega} \frac{e^{-x/k}}{x} \, d\mathbf{x}' = k^2 - k^2 \frac{a_3}{2} \int_0^{\infty} (D \times A) \, du \quad (\text{A.3})$$

where

$$D = \frac{1}{(u + a_3^2)^{3/2}} \left(1 + \frac{a}{k} \sqrt{\frac{u + a_3^2}{u + a^2}} \right) \exp \left(-\frac{a}{k} \sqrt{\frac{u + a_3^2}{u + a^2}} \right),$$

$$A = I_0(B\rho) \cosh(Cz), \quad B = \frac{1}{k} \sqrt{\frac{u}{u + a^2}}, \quad C = \frac{a}{k\sqrt{u + a^2}}$$

$$u = a_3^2 \tan^2 \theta, \quad \rho = \sqrt{x_1^2 + x_2^2}$$

I_M is the M th order modified Bessel function of the first kind, a and a_3 are the half-length of transverse and major axis of the ellipsoidal inclusion. The major axis of the ellipsoid lines with the axis z . The derivatives of Eq. (A.3) read

$$M_{,i}(\mathbf{x}, k) = -\frac{a_3}{2} k^2 \int_0^{\infty} (D \times A_{,i}) \, du \quad (\text{A.4a})$$

$$M_{,ij}(\mathbf{x}, k) = -\frac{a_3}{2} k^2 \int_0^{\infty} (D \times A_{,ij}) \, du \quad (\text{A.4b})$$

$$M_{,ijm}(\mathbf{x}, k) = -\frac{a_3}{2} k^2 \int_0^{\infty} (D \times A_{,ijm}) \, du \quad (\text{A.4c})$$

$$M_{,ijmn}(\mathbf{x}, k) = -\frac{a_3}{2} k^2 \int_0^{\infty} (D \times A_{,ijmn}) \, du \quad (\text{A.4d})$$

where

$$A_{,x} = B \cosh(Cz) I_1(B\rho) \frac{x_x}{\rho}$$

$$\begin{aligned} A_{,\alpha\beta} &= B \cosh(Cz) \frac{1}{2\rho^3} [B\rho [I_0(B\rho) + I_2(B\rho)] x_{\alpha} x_{\beta} \\ &\quad + 2I_1(B\rho) (\rho^2 \delta_{\alpha\beta} - x_{\alpha} x_{\beta})] \end{aligned}$$

$$A_{,\alpha\beta\gamma} = B \cosh(Cz)$$

$$\begin{aligned} &\times \left\{ \left[-\frac{3B}{2\rho^4} x_{\alpha} x_{\beta} x_{\gamma} + \frac{B}{2\rho^2} (\delta_{\alpha\beta} x_{\gamma} + \delta_{\alpha\gamma} x_{\beta} + \delta_{\gamma\beta} x_{\alpha}) \right] I_0(B\rho) \right. \\ &\quad + \left[\frac{3}{\rho^5} x_{\alpha} x_{\beta} x_{\gamma} + \frac{3B^2}{4\rho^3} x_{\alpha} x_{\beta} x_{\gamma} - \frac{1}{\rho^3} (\delta_{\alpha\beta} x_{\gamma} + \delta_{\alpha\gamma} x_{\beta} + \delta_{\gamma\beta} x_{\alpha}) \right] I_1(B\rho) \\ &\quad + \left[-\frac{3B}{2\rho^4} x_{\alpha} x_{\beta} x_{\gamma} + \frac{B}{2\rho^2} (\delta_{\alpha\beta} x_{\gamma} + \delta_{\alpha\gamma} x_{\beta} + \delta_{\gamma\beta} x_{\alpha}) \right] I_2(B\rho) \\ &\quad \left. + \left[\frac{B^2}{4\rho^3} x_{\alpha} x_{\beta} x_{\gamma} \right] I_3(B\rho) \right\} \end{aligned}$$

$$\begin{aligned}
 A_{,\alpha\beta\gamma\lambda} = & B \cosh(Cz) \times \left\{ \frac{B}{\rho^6} \left[\frac{15}{2} x_\alpha x_\beta x_\gamma x_\lambda + \frac{3}{8} B^2 \rho^2 x_\alpha x_\beta x_\gamma x_\lambda \right. \right. \\
 & - \frac{3}{2} \rho^2 x_\lambda (\delta_{\alpha\beta} x_\gamma + \delta_{\alpha\gamma} x_\beta + \delta_{\gamma\beta} x_\alpha) \\
 & - \frac{3}{2} \rho^2 (\delta_{\alpha\lambda} x_\beta x_\gamma + \delta_{\beta\lambda} x_\alpha x_\gamma + \delta_{\gamma\lambda} x_\beta x_\alpha) \\
 & \left. \left. + \frac{\rho^4}{2} (\delta_{\alpha\beta} \delta_{\gamma\lambda} + \delta_{\alpha\gamma} \delta_{\beta\lambda} + \delta_{\alpha\lambda} \delta_{\gamma\beta}) \right] I_0(B\rho) \right. \\
 & + \frac{1}{\rho^7} \left[-\frac{9}{2} B^2 \rho^2 x_\alpha x_\beta x_\gamma x_\lambda - 15 x_\alpha x_\beta x_\gamma x_\lambda \right. \\
 & + \frac{3}{4} B^2 \rho^4 x_\lambda (\delta_{\alpha\beta} x_\gamma + \delta_{\alpha\gamma} x_\beta + \delta_{\gamma\beta} x_\alpha) \\
 & + 3 \rho^2 x_\lambda (\delta_{\alpha\beta} x_\gamma + \delta_{\alpha\gamma} x_\beta + \delta_{\gamma\beta} x_\alpha) \\
 & + 3 \rho^2 (\delta_{\alpha\lambda} x_\beta x_\gamma + \delta_{\beta\lambda} x_\alpha x_\gamma + \delta_{\gamma\lambda} x_\beta x_\alpha) \\
 & \left. \left. + \frac{3}{4} B^2 \rho^4 (\delta_{\alpha\lambda} x_\beta x_\gamma + \delta_{\beta\lambda} x_\alpha x_\gamma + \delta_{\gamma\lambda} x_\beta x_\alpha) \right. \right. \\
 & \left. \left. - \rho^4 (\delta_{\alpha\beta} \delta_{\gamma\lambda} + \delta_{\alpha\gamma} \delta_{\beta\lambda} + \delta_{\alpha\lambda} \delta_{\gamma\beta}) \right] \right. \\
 & \times I_1(B\rho) + \frac{B}{\rho^6} \left[\frac{15}{2} x_\alpha x_\beta x_\gamma x_\lambda + \frac{B^2 \rho^2}{2} x_\alpha x_\beta x_\gamma x_\lambda \right. \\
 & - \frac{3}{2} \rho^2 x_\lambda (\delta_{\alpha\beta} x_\gamma + \delta_{\alpha\gamma} x_\beta + \delta_{\gamma\beta} x_\alpha) \\
 & - \frac{3}{2} \rho^2 (\delta_{\alpha\lambda} x_\beta x_\gamma + \delta_{\beta\lambda} x_\alpha x_\gamma + \delta_{\gamma\lambda} x_\beta x_\alpha) \\
 & \left. \left. + \frac{\rho^4}{2} (\delta_{\alpha\beta} \delta_{\gamma\lambda} + \delta_{\alpha\gamma} \delta_{\beta\lambda} + \delta_{\alpha\lambda} \delta_{\gamma\beta}) \right] I_2(B\rho) \right. \\
 & + \frac{B^2}{\rho^5} \left[-\frac{3}{2} x_\alpha x_\beta x_\gamma x_\lambda + \frac{\rho^2}{4} x_\lambda (\delta_{\alpha\beta} x_\gamma + \delta_{\alpha\gamma} x_\beta + \delta_{\gamma\beta} x_\alpha) \right. \\
 & \left. \left. + \frac{\rho^2}{4} (\delta_{\alpha\lambda} x_\beta x_\gamma + \delta_{\beta\lambda} x_\alpha x_\gamma + \delta_{\gamma\lambda} x_\beta x_\alpha) \right] I_3(B\rho) \right. \\
 & \left. \left. + \frac{B^3}{\rho^4} \left[\frac{1}{8} x_\alpha x_\beta x_\gamma x_\lambda \right] I_4(B\rho) \right\}
 \end{aligned}$$

The indices $\alpha, \beta, \gamma, \lambda$ range from 1 to 2, and

$$\begin{aligned}
 A_{,z} &= C \sinh(Cz) I_0(B\rho) \\
 A_{,zz} &= C^2 \cosh(Cz) I_0(B\rho), \quad A_{,\alpha z} = (A_{,\alpha})_{,z}, \\
 A_{,zzz} &= C^3 \sinh(Cz) I_0(B\rho), \quad A_{,\alpha zz} = (A_{,\alpha})_{,zz}, \\
 A_{,\alpha\beta z} &= (A_{,\alpha\beta})_{,z}, \\
 A_{,zzzz} &= C^4 \cosh(Cz) I_0(B\rho), \quad A_{,\alpha zzz} = (A_{,\alpha})_{,zzz}, \\
 A_{,\alpha\beta zz} &= (A_{,\alpha\beta})_{,zz}, \quad A_{,\alpha\beta\gamma z} = (A_{,\alpha\beta\gamma})_{,z}
 \end{aligned}$$

With the previous expression, the micropolar Eshelby tensors and their average over the ellipsoidal domain can be calculated.

Appendix B. Method of orientational average

B.1. 3D randomly oriented inclusions

Adopting Wapole notation [36], a transversely isotropic tensor A , whose local symmetric axis is x_3 , can be expressed as

$$A = (c, g, h, d, e, f) \quad (\text{B.1})$$

its corresponding matrix form is

$$A = \begin{bmatrix} \frac{c+f}{2} & \frac{c-f}{2} & g & 0 & 0 & 0 \\ \frac{c-f}{2} & \frac{c+f}{2} & g & 0 & 0 & 0 \\ h & h & d & 0 & 0 & 0 \\ 0 & 0 & 0 & e & 0 & 0 \\ 0 & 0 & 0 & 0 & e & 0 \\ 0 & 0 & 0 & 0 & 0 & f \end{bmatrix} \quad (\text{B.2})$$

The orientational average in 3D space is defined as

$$\bar{A} = \langle T^{-1}AT \rangle = \frac{1}{2\pi} \int_0^\pi \int_0^{2\pi} T^{-1}AT \sin\theta d\theta d\phi \quad (\text{B.3})$$

where T is the transform matrix of a second-order tensor between two coordinate frames. Then the 3D orientational average of A is isotropic:

$$\bar{A} = \left(2\delta + \frac{2}{3}\beta, \delta - \frac{2}{3}\beta, \delta - \frac{2}{3}\beta, \delta + \frac{4}{3}\beta, 2\beta, 2\beta \right) \quad (\text{B.4})$$

with

$$\begin{aligned}
 \delta &= \frac{1}{9}(2c + 2g + 2h + d), \\
 \beta &= \frac{1}{30}[c - 2(g + h) + 2d + 6(e + f)]
 \end{aligned} \quad (\text{B.5})$$

B.2. In-plane randomly oriented inclusions

Assuming the inclusions are randomly oriented in global x_2 - x_3 plane, the in-plane average of A is transversely isotropic, and its symmetric axis is x_1 :

$$\bar{A}_{x_1} = \langle T^{-1}AT \rangle = \frac{1}{\pi} \int_0^\pi T^{-1}AT d\theta = (\bar{c}, \bar{g}, \bar{h}, \bar{d}, \bar{e}, \bar{f}) \quad (\text{B.6})$$

Its matrix form is

$$\bar{A}_{x_1} = \begin{bmatrix} \bar{d} & \bar{g} & \bar{g} & 0 & 0 & 0 \\ \bar{h} & \frac{\bar{c}+\bar{f}}{2} & \frac{\bar{c}-\bar{f}}{2} & 0 & 0 & 0 \\ \bar{h} & \frac{\bar{c}-\bar{f}}{2} & \frac{\bar{c}+\bar{f}}{2} & 0 & 0 & 0 \\ 0 & 0 & 0 & \bar{f} & 0 & 0 \\ 0 & 0 & 0 & 0 & \bar{e} & 0 \\ 0 & 0 & 0 & 0 & 0 & \bar{e} \end{bmatrix} \quad (\text{B.7})$$

where

$$\begin{aligned}
 \bar{c} &= \frac{1}{8}[2(c + f) + 4(h + g + d)], \\
 \bar{g} &= \frac{c-f}{4} + \frac{g}{2}, \quad \bar{h} = \frac{c-f}{4} + \frac{h}{2}, \\
 \bar{d} &= \frac{c+f}{2}, \quad \bar{e} = \frac{e+f}{2}, \\
 \bar{f} &= \frac{1}{8}[c + f - 2(g + h - d) + 4e]
 \end{aligned} \quad (\text{B.8})$$

References

- [1] N.A. Fleck, G.M. Muller, M.F. Ashby, J.W. Hutchinson, Strain gradient plasticity: theory and experiment, *Acta Metall. Mater.* 42 (1993) 475–487.
- [2] M. Kouzeli, A. Mortensen, Size dependent strengthening in particle reinforced aluminium, *Acta Mater.* 50 (2002) 39–51.
- [3] G.K. Hu, X.N. Liu, T.J. Lu, A variational method for nonlinear micropolar composite, *Mech. Mater.* 37 (2005) 407–425.
- [4] A.V. Cherkov, K.A. Lurie, G.W. Milton, Invariant properties of the stress in plane elasticity and equivalence classes of composites, *Proc. R. Soc. Lond. A* 438 (1992) 519–529.
- [5] S. Nemat-Nasser, M. Hori, *Micromechanics: Overall Properties of Heterogeneous Materials*, Elsevier, North-Holland, 1993.
- [6] S. Torquato, Random heterogeneous media: microstructure and improve bounds on effective properties, *Appl. Mech. Rev.* 44 (1991) 37–75.
- [7] G.K. Hu, G.J. Weng, Connection between the double inclusion model and the Ponte Castañeda–Willis, Mori–Tanaka, and Kuster–Toksoz model, *Mech. Mater.* 32 (2000) 495–503.
- [8] S. Schmauder, Computational mechanics, *Ann. Rev. Mater. Res.* 32 (2002) 437–465.
- [9] A.C. Eringen, Theory of micropolar elasticity, in: H. Leibowitz (Ed.), *Fracture, an Advanced Treatise*, Academic Press, New York, 1968.
- [10] H.B. Muhlhaus, I. Vardoulakis, The thickness of shear bands in granular materials, *Geotechnique* 37 (1987) 271–283.
- [11] R. de Borst, A generalization of J2-flow theory for polar continua, *Comput. Methods Appl. Mech. Eng.* 103 (1993) 347–362.
- [12] A.C. Eringen, *Microcontinuum Field Theory*, Springer, New York, 1999.
- [13] N.A. Fleck, J.W. Hutchinson, A phenomenological theory for strain gradient effect in plasticity, *J. Mech. Phys. Solids* 41 (12) (1993) 1825–1857.
- [14] E.C. Aifantis, On the microstructural origin of certain inelastic models, *Trans. ASME J. Eng. Mater. Technol.* 106 (1984) 326–330.
- [15] H. Gao, Y. Huang, W.D. Nix, J.W. Hutchinson, Mechanism-based strain gradient plasticity—I. Theory, *J. Mech. Phys. Solids* 47 (1999) 1239–1263.
- [16] V.P. Smyshlyaev, N.A. Fleck, Bounds and estimates for linear composites with strain gradient effects, *J. Mech. Phys. Solids* 42 (1994) 1851–1882.
- [17] V.P. Smyshlyaev, N.A. Fleck, Bounds and estimates for the overall plastic behavior of composites with strain gradient effects, *Proc. R. Soc. Lond. A* 451 (1995) 795–810.
- [18] N.A. Fleck, J.R. Willis, Bounds and estimates for the effect of strain gradient upon the effective plastic properties of an isotropic two-phase composite, *J. Mech. Phys. Solids* 52 (2004) 1855–1888.
- [19] X. Yuan, Y. Tomita, Effective properties of Cosserat composites with periodic microstructure, *Mech. Res. Commun.* 28 (3) (2001) 265–270.
- [20] S. Chen, T.C. Wang, Size effects in the particle-reinforced metal-matrix composites, *Acta Mech.* 157 (1–4) (2002) 113–127.
- [21] Z.Q. Cheng, L.H. He, Micropolar elastic fields due to a spherical inclusion, *Int. J. Eng. Sci.* 33 (3) (1995) 389–397.
- [22] Z.Q. Cheng, L.H. He, Micropolar elastic fields due to a circular cylindrical inclusion, *Int. J. Eng. Sci.* 35 (7) (1997) 659–668.
- [23] P. Sharma, A. Dasgupta, Average elastic field and scale-dependent overall properties of heterogeneous micropolar materials containing spherical and cylindrical inhomogeneities, *Phys. Rev. B* 66 (2002) 1–10.
- [24] X.N. Liu, G.K. Hu, A continuum micromechanical theory of overall plasticity for particulate composites including particle size effect, *Int. J. Plasticity* 21 (2005) 777–799.
- [25] F. Xun, G.K. Hu, Z.P. Huang, Effective in plane moduli of composites with a micropolar matrix and coated fiber, *Int. J. Solids Struct.* 41 (2004) 247–265.
- [26] F. Xun, G.K. Hu, Z.P. Huang, Size-dependence of overall in-plane plasticity for fiber composites, *Int. J. Solids Struct.* 41 (2004) 4713–4730.
- [27] Y.P. Qiu, G.J. Weng, A theory of plasticity for porous materials and particle-reinforced composites, *Int. J. Plasticity* 9 (1992) 261–268.
- [28] P. Suquet, Overall properties of nonlinear composites: a modified secant moduli theory and its link with Ponte Castañeda’s nonlinear variational procedure, *C.R. Acad. Sci. Paris Ser., II* 320 (1995) 563–571.
- [29] G.K. Hu, A method of plasticity for general aligned spheroidal void or fiber-reinforced composites, *Int. J. Plasticity* 12 (1996) 439–449.
- [30] P. Castañeda, The effective mechanical properties of nonlinear isotropic composite, *J. Mech. Phys. Solids* 39 (1991) 45–71.
- [31] H.S. Ma, G.K. Hu, Eshelby tensors for an ellipsoidal inclusion in a micropolar medium, *Int. J. Eng. Sci.*, in press.
- [32] H.S. Ma, G.K. Hu, Influence of fiber’s shape and size on overall elastoplastic property for micropolar composites, *Int. J. Solids Struct.*, in press.
- [33] W. Nowacki, *Theory of Asymmetric Elasticity*, Pergamon Press, New York, 1986.
- [34] T. Mura, *Micromechanics of Defects in Solids*, Martinus Nijhoff, Netherlands, 1982.
- [35] T. Mori, K. Tanaka, Average stress in matrix and average elastic energy of materials with misfitting inclusions, *Acta Metall. Mater.* 21 (1973) 571–573.
- [36] L.J. Wapole, On the overall elastic moduli of composite materials, *J. Mech. Phys. Solids* 17 (1969) 235–251.
- [37] G.P. Tandon, G.J. Weng, Average stress in the matrix and effective moduli of randomly oriented composites, *Compos. Sci. Technol.* 27 (1986) 111–132.